4-2020

Surface Elevation and Sedimentation Dynamics in the Ganges-Brahmaputra Tidal Delta Plain, Bangladesh: Evidence for Mangrove Adaptation to Human-Induced Tidal Amplification

Edwin J. Bomer

Carol A. Wilson

Richard Hale

Abu Naser Mohsin Hossain

F.M. Arifur Rahman

Catena 187 (2020) 104312

Contents lists available at ScienceDirect

Catena

journal homepage: www.elsevier.com/locate/catena

Surface elevation and sedimentation dynamics in the Ganges-Brahmaputra tidal delta plain, Bangladesh: Evidence for mangrove adaptation to human-induced tidal amplification

Edwin J. Bomer[a,b,*], Carol A. Wilson[a,b], Richard P. Hale[c], Abu Naser Mohsin Hossain[d], F.M. Arifur Rahman[e]

[a] Department of Geology and Geophysics, Louisiana State University, Baton Rouge, LA, USA
[b] Coastal Studies Institute, Louisiana State University, Baton Rouge, LA, USA
[c] Department of Ocean, Earth & Atmospheric Sciences, Old Dominion University, Norfolk, VA, USA
[d] Bangladesh Forest Department, Dhaka, Bangladesh
[e] Department of Geology, University of Dhaka, Dhaka, Bangladesh

ARTICLE INFO

Keywords:
Surface elevation
Vertical accretion
Shallow subsidence
Mangroves
Sea-level rise
Sundarbans
Bangladesh

ABSTRACT

In the Ganges-Brahmaputra (G-B) delta, periodic flooding of the land surface during the tidal cycle coupled with enormous sediment delivery during the monsoon promotes sediment accretion and surface elevation gain through time. However, over the past several decades, widespread embankment ("polder") construction in the G-B tidal delta plain has led to numerous environmental disturbances, including channel siltation and tide range amplification. While previous research indicates that rates of sediment accretion are relatively high in the G-B tidal delta plain, it remains unclear if and how surface elevation is maintaining pace with relative sea-level rise (RSLR) in this region. In this study, we utilize an array of surface elevation tables, sediment traps, and groundwater piezometers to provide longitudinal trends of sedimentation and elevation dynamics with respect to local platform elevation and associated hydroperiod. Two hydro-geomorphic settings of the Sundarbans mangrove forest are compared: higher elevation stream-bank and lower elevation interior. Seasonal measurements over a time span of 5 years reveal that elevation gain is occurring in all settings, with the highest rates observed at elevated stream-bank zones. Elevation gain occurs primarily in response to sediment accretion, with possible minor contributions from pore-water storage and swelling of clay minerals during the monsoon season (i.e., belowground biomass and organic contribution is minimal). As a result, elevation loss and shallow subsidence in the G-B delta is unlikely to be caused by compaction of organic-rich soils, but rather appears to be controlled by seasonal lowering of the groundwater table and compaction of clay minerals. Rates of surface elevation gain in the Sundarbans greatly exceed rates of RSLR and more closely follow rates of RSLR augmented from tide range amplification, indicating that this landscape is adapting to human-induced environmental change. The proceedings of this study underscore the adaptability of the natural G-B tidal delta plain to local environmental disturbances, with the caveat that these defenses may be lost to future upstream reductions in sediment supply.

1. Introduction

The unhindered deposition of detrital and organic material is crucial for maintaining surface equilibrium in low-lying coastal margins (Nicholls et al., 2007; Syvitski et al., 2009; Vörösmarty et al., 2009), especially given the prospect of accelerated eustatic sea-level rise (Church and White, 2006; Jevrejeva et al., 2008). However, recent research in a variety of delta systems, including the Mississippi (Meade and Moody, 2010), Ganges-Brahmaputra (Auerbach et al., 2015a), Nile (McManus, 2002) and Yellow (Wang et al., 2007), has provided numerous examples of how man-made river control structures stagnate, or in some cases, completely prevent sediment delivery to the floodplain. These anthropogenic modifications to the landscape also alter river channel hydrodynamics, leading to deleterious effects like channel siltation (Wolanski et al., 2001; Wilson et al., 2017) and tide range amplification (Pethick and Orford, 2013). While restorative techniques are

* Corresponding author at: Department of Geology and Geophysics, Louisiana State University, Baton Rouge, LA, USA.
E-mail address: ebomer1@lsu.edu (E.J. Bomer).

https://doi.org/10.1016/j.catena.2019.104312
Received 28 May 2019; Received in revised form 21 September 2019; Accepted 4 October 2019
Available online 25 November 2019

currently being developed and implemented in some coastal communities (e.g., Mississippi River Delta, Peyronnin et al., 2013), it is well accepted that the interplay of hydrodynamics, sediment deposition, and landscape evolution can differ substantially among deltaic systems (Orton and Reading, 1993; Syvitski and Saito, 2007). Thus, site-specific consideration of these geomorphic processes, in addition to understanding the degree of human-induced modification, is critical for properly assessing the sustainability of the system and for formulating restoration initiatives that balance environmental, economic, and humanitarian interests.

Among delta systems worldwide, the Ganges-Brahmaputra (G-B) delta is considered to be one of the most vulnerable to the effects of climate change, owing in large part to anthropogenic stressors (Syvitski et al., 2009; Tessler et al., 2015; Higgins et al., 2018). Indeed, the G-B delta, with a burgeoning population of ~144 million, is the most populated delta on Earth (Higgins, 2016). In Bangladesh, which occupies roughly 70% of the G-B delta, a significant proportion of the population lives at or near sea level, placing millions of inhabitants at risk of inundation from rising sea levels as well as cyclone-induced storm surges. In an effort to mitigate these environmental hazards, the Bangladesh government began constructing earthen embankments along channel margins in low-lying agrarian regions of the country in the 1960s (Alam, 1996; Allison, 1998; Islam, 2006). Cultivated land within these embankments, hereafter referred to by the Dutch term "polder," also benefitted from augmented rice production due to prevention of saline water intrusion during the dry season. However, it is now widely recognized that polderization has contributed to a variety of deleterious outcomes that affect communities both in the vicinity and far from their construction.

For instance, Pethick and Orford (2013) compared long-term tide gauge records from three stations located in the Passur Estuary (see Fig. 1A for location) and found that the rate of change of mean high water level exceeded that of mean sea level between 1968 and 2011, indicating that an increase in tidal range had occurred over this time span (e.g., from ~1.4 to ~2.3 m at Khulna). The timing of tidal range amplification and observation that the magnitude of change was particularly high near poldered regions suggested that embankment construction and resultant reduction of the tidal prism were the causal mechanisms. A subsequent study found the closure of 1500 km of tidal channels reroutes 1.4 km^3 of water (Wilson et al., 2017). Accordingly, if the effects of human alteration are not considered (e.g., tidal amplification in this case), rates of sea-level rise can be substantially underestimated (Kirwan and Megonigal, 2013; Pethick and Orford, 2013). These findings underscore the notion that eustatic sea-level rise and subsidence are not the only processes affecting the surface equilibrium of coastal systems, as delta floodplains aggrade to mean flood elevation (Törnqvist and Bridge, 2002) and tidal landscapes build to approximately mean high water (MHW, Kirwan and Guntenspergen, 2010).

Situated adjacent to the poldered landscape is the Sundarbans National Park (hereafter referred to as the Sundarbans), a pristine and expansive mangrove forest that spans ~10,000 km^2 (Fig. 1A). The Sundarbans holds importance for coastal populations as the mangrove ecosystem offers a wide range of ecological resources (e.g., fish, crabs, timber, and honey) and provides a natural buffer from storm surges and tidal bores (e.g., Van Coppenolle et al., 2018). Although it is recognized that poldered regions exist at an elevation deficit relative to the surrounding natural tidal platforms (Auerbach et al., 2015a; Rogers and Overeem, 2017), the vulnerability of the natural G-B tidal delta plain and Sundarbans forest to inundation from sea-level rise is presently unclear. Loucks et al. (2010) indicate progressive submergence of the Sundarbans with increasing sea level ("bathtub model"), particularly in excess of 20 cm of sea-level rise and in low-lying areas of the forest interior. Conversely, other researchers contend that the Sundarbans is geomorphically stable based on observed sediment accretion rates that approximate the local rate of relative sea-level rise (~1 cm yr^{-1}, Allison and Kepple, 2001; Rogers et al., 2013). Ultimately, however, the fate of coastal wetlands is controlled by the maintenance of surface elevation, and numerous studies have shown that shallow subsidence

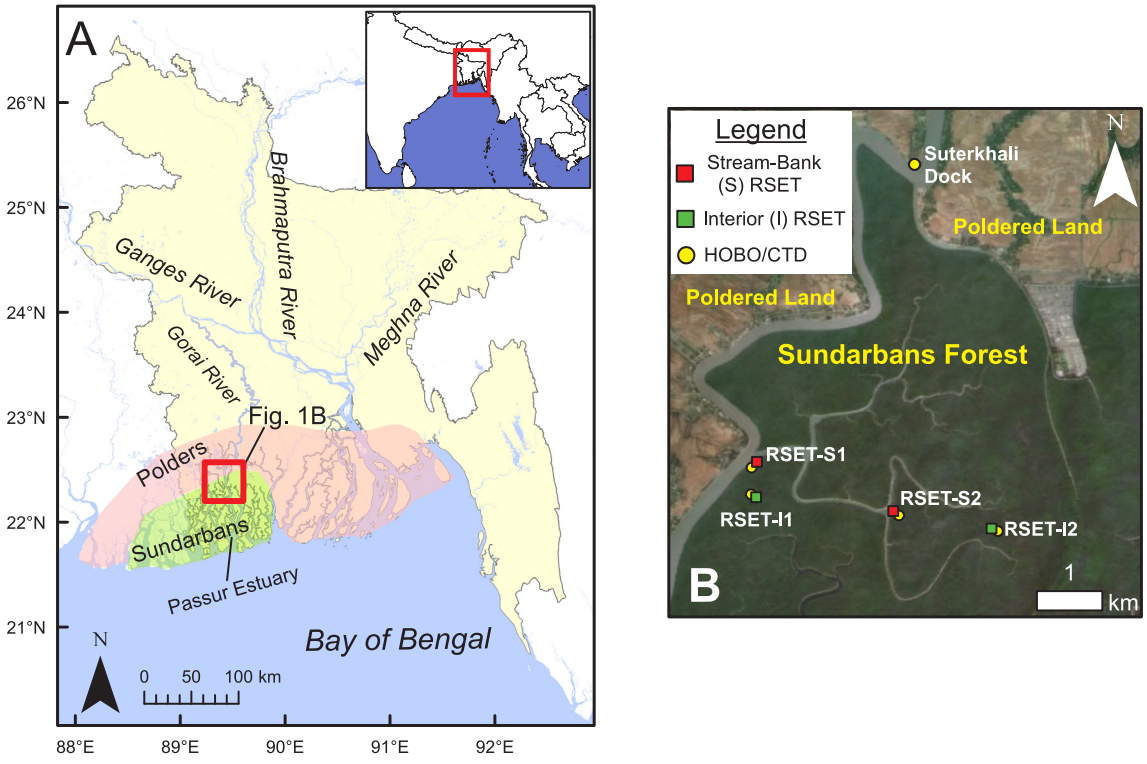

Fig. 1. (A) Physiographic map of greater Bangladesh with the Sundarbans mangrove forest and poldered areas outlined in green and pink, respectively; (B) rod surface elevation table (RSET) and hydrologic instrument coverage in the field area. (For interpretation of the references to color in this figure legend, the reader is referred to the web version of this article.)

and RSLR can outpace gains from accretion (e.g., Cahoon and Hensel, 2006; Rogers et al., 2006; Krauss et al., 2010; Lovelock et al., 2011). Rates of surface elevation change, in conjunction with the forcing components (e.g., tidal hydroperiod, sedimentation dynamics), are therefore critical to accurately assess the sustainability of the G-B tidal delta plain and other coastal systems worldwide.

This study reports the first longitudinal data (i.e., seasonal measurements over a time span of 5 years) on elevation and sedimentation dynamics in the natural G-B tidal delta plain, using a modified version of the widely applied surface elevation table-marker horizon methodology (e.g., Cahoon et al., 2002). Understanding seasonal and interannual changes in surface elevation is vital for informed decisions on land management (World Bank, 2015), a topic that remains a matter of debate in coastal Bangladesh (Hossain et al., 2015; Auerbach et al., 2015b). Thus, the specific objectives of this study are to: (1) document surface elevation and sediment accretion change in different hydrogeomorphic landscapes of the natural G-B tidal delta plain, (2) ascertain the importance of seasonal processes on elevation and accretion dynamics, (3) identify surficial and below-ground processes that govern these changes, and (4) determine whether the landscapes are sustainable with respect to sea-level rise and human-induced tidal amplification.

2. Study area

Originating in the greater Himalaya, the Ganges and Brahmaputra rivers flow south through India and coalesce in central Bangladesh. Water discharge and sediment load of these rivers are strongly regulated by climatic conditions, the most notable of which being the South Asian monsoon (e.g., Coleman, 1969). From June through September, southwest winds blow onshore from the Bay of Bengal, triggering persistent rainfall and flooding throughout the Indian subcontinent. The annual deluge is largely responsible for delivering 1270 km^3 of water and 1060 Mt of sediment to the G-B delta and Indian Ocean each year, representing one of the largest fluvial sediment loads in the world (Milliman and Farnsworth, 2011 and references therein). Integrated satellite imagery analyses and field observations on the inner continental shelf indicate that the direction of the residual current and sediment transport is landward and to the west (Barua et al., 1994). Nearshore waves and tides then advect these turbid waters inland through a dense network of tidal channels, dispersing sediments throughout the lower tidal delta plain (Hale et al., 2019a). This sediment conveyance pathway allows areas that are no longer directly connected with fluvial point sources to maintain vertical accretion in accordance with rising sea level (Rogers et al., 2013).

Within the greater G-B delta system, the present study is focused on the tide-dominated, lower delta plain (range = 2–4 m, BIWTA, 2019; see also Fig. 1A). Located ~150 km west of the river mouth, the G-B tidal delta plain was the active lobe of the delta prior to periodic, eastward avulsions of the main-stem Ganges and Brahmaputra rivers during the late Holocene (Allison et al., 2003). Today, the tidal delta plain is less connected to fluvial input: the Gorai River is the only source of fresh water to the region and has decreased in mean discharge by 95% over the past ~50 years partly due to the construction of the Farakka barrage (Mirza, 1998; EGIS, 2000; Shaha and Cho, 2016) and partly due to natural infilling of the Ganges-Gorai distributary off-take (Pethick, 2012; Winterwerp and Giardino, 2012). Like much of Bangladesh, the lower delta plain experiences a tropical monsoonal climate, which is characterized by mean high and low temperatures of 31 and 22 °C, respectively, and mean annual precipitation in excess of 1800 mm. Areas that have not been cleared for agricultural purposes are dominated by an assemblage of mangroves that includes Sundari (*Heritiera fomes*), Gewa (*Excoecaria agallocha*), Kankra (*Bruguiera decandra*), and Bain (*Avicennia marina*) species (Giri et al., 2014). Sediment cores taken across the lower delta plain to ~5 m depth reveal that the shallow subsurface typically consists of fining-upward successions of mud-rich sand to rooted silts and clays (Allison et al., 2003).

3. Methods

3.1. Surface elevation change

Inter-annual surface elevation change was recorded using an array of rod surface elevation table (RSET) instruments (Fig. 1B, 2, see also Tables S1 and S2 in Supplementary Materials for installation details and measurement dates). During RSET installation, stainless steel rods (15 mm in diameter, 1.22 m in length) were driven into the substrate until refusal and cemented within 10-cm diameter PVC pipes for stability. The depth of the benchmark ranged from 12.2 to 18.3 m, depending on the local depth of the incompressible substrate (i.e., consolidated sand). Following the procedures of Cahoon et al. (2002), nine measurements of surface elevation were taken at eight different positions for a total of 72 measurements at each site. During data collection, any natural obstructions (e.g., tree roots, pneumatophores) or bioturbation features (e.g., crab mounds, footprints) that interfered with the true ground surface were noted, and the associated measurements were omitted during analysis. RSET stations were established in two hydro-geomorphic settings in the Sundarbans mangrove forest: 1) within close proximity (~10 m) of a tidal channel and typically slightly higher elevation, termed “stream-bank (S),” and 2) distal (> 100 m) from any tidal channel and typically at lower platform elevation, termed “interior (I)” (Fig. 1B; Table 1). RSET instruments were deployed in two phases: RSET-S1 and I1 were installed in May 2014, while RSET-S2 and I2 were installed in October 2015. Baseline measurements were taken at least a month after deployment to allow for any disturbance during installation to have recovered. Due to differences in deployment periods, RSET results reported by hydro-geomorphic setting were averaged when instrument deployment periods coincided (e.g., RSET-S1 and S2 between October 2015 and March 2019) and were reported individually when they did not coincide (e.g., RSET-S1 between May 2014 and October 2015).

Table 1
Mean annual rates (± standard error) of surface elevation, vertical accretion measured by sediment tiles (ST) and marker horizons (MH), and shallow subsidence among study sites. Shallow subsidence values are based on the difference between surface elevation change and vertical accretion from the sediment tile method, when available. Shallow subsidence errors are propagated from the surface elevation and vertical accretion error component pools.

Station	Landscape	Record Duration (yr)	Surface Elevation Change (cm yr^{-1})	Vertical Accretion – ST (cm yr^{-1})	Vertical Accretion – MH (cm yr^{-1})	Shallow Subsidence (cm yr^{-1})
RSET-S1	Stream-Bank	5.0	2.59 ± 0.17	3.29 ± 0.29	3.64 ± 1.18	0.70 ± 0.46
RSET-I1	Interior	5.0	1.40 ± 0.14	2.62 ± 0.28	2.78 ± 1.01	1.22 ± 0.42
RSET-I2	Interior	3.5	1.05 ± 0.22	1.76 ± 0.29	2.32 ± 0.73	0.71 ± 0.51
RSET-S2	Stream-Bank	3.5	1.16 ± 0.37	3.00 ± 0.31	3.00 ± 0.57	1.84 ± 0.68
Average	Stream-Bank	5.0	2.16 ± 0.26	3.29 ± 0.24	3.32 ± 0.88	1.13 ± 0.50
Average	Interior	5.0	1.32 ± 0.17	2.12 ± 0.20	2.55 ± 0.87	0.80 ± 0.37

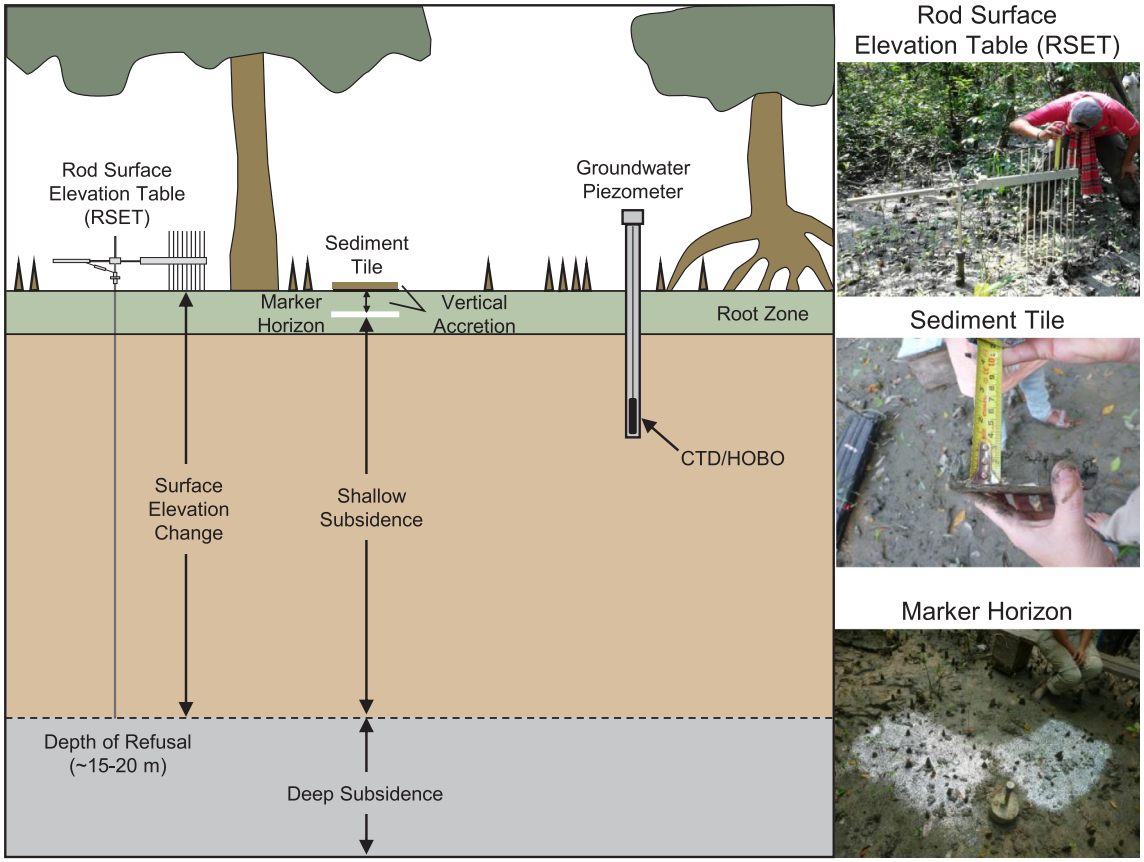

Fig. 2. Schematic diagram (not to scale) of methods employed in this study (modified from Cahoon et al., 2002). RSETs, marker horizons (either brick dust or plastic glitter), sediment tiles, and piezometers were deployed within the Sundarbans forest.

3.2. Vertical accretion

Seasonal sediment vertical accretion was directly measured using two methods: sediment tiles and marker horizons (Fig. 2). As recommended by Steiger et al. (2003), these two techniques were used together to provide quality control in this dynamic depositional setting. Following the approach of Rogers et al. (2013), four ceramic sediment tiles (area = 100 cm^2), were placed on the ground surface in the vicinity of each RSET station (Fig. 2). Following a deployment period of ~6 months, tiles were excavated and vertical accretion was measured at two points on each side of the tile for a total of eight measurements per tile (Fig. 2). The average of all measurements (n = 32, when all tiles were found) was calculated to obtain the amount of seasonal accretion. During data collection, any evidence of faunal disturbance (e.g., broken tile, crab mounding) was noted and associated measurements were omitted during analysis. Tiles were cleared of sediments following each sampling period and re-deployed in the same location for consistency and to facilitate identification in subsequent data collection periods.

Sediment accretion as recorded by tiles was supplemented with artificial marker horizons (Cahoon and Turner, 1989; Fig. 2). Brick dust or plastic glitter was dispersed on the ground surface in two plots (area ≈ 1 m^2) situated on different sides of the RSET receiver (Fig. 2, Table S1). During subsequent field excursions, small cubic cores (~4 cm^2) were excavated in undisturbed locations to locate marker horizons and quantify sediment accretion. The distance from the ground surface to the marker horizon was calculated as the amount of vertical accretion that had occurred during the deployment period. Additionally, the vertical distribution and order of markers in the subsurface was noted and used to assess the degree of bioturbation.

3.3. Shallow subsidence

Comparisons of surface elevation and vertical accretion trends can be used to quantify shallow subsidence, adapted from Cahoon et al. (1995) as:

$$SS = VA - SEC \quad (1)$$

where SS is calculated shallow subsidence, VA is measured vertical accretion, and SEC is measured surface elevation change. Positive values of SS indicate that shallow subsidence occurred at depth between the ground surface and the depth of refusal for the RSET rods (see Fig. 2, Table S1), whereas negative values indicate shallow subsurface expansion has occurred. SS values close to zero indicate that surface elevation change is occurring primarily as a function of sediment accretion, with negligible shallow subsidence or expansion (see Cahoon, 2015).

3.4. Platform flooding

Local surface and groundwater hydrodynamic data were obtained from Schlumberger Diver CTD (conductivity, temperature, and pressure) and Onset U20L-01 HOBO (water pressure) instruments attached to a dock piling in a nearby tidal channel (n = 1; surface water) and emplaced in piezometers on the platforms near the RSET instruments (n = 4; groundwater piezometers screened from the surface to a depth of 2 m) (Figs. 1B, 2). The instruments logged data every 10 min to document water level, water temperature, and electrical conductivity (a proxy for salinity) changes over tidal and seasonal time scales. Mangrove platform flooding events were identified in the hydrograph data by a rapid increase in water pressure followed by a gradual decline in pressure as waters receded from the platform. Seasonal duration of

platform inundation (i.e., hydroperiod) was quantified at two locations (RSET-S1 and RSET-I1) by tabulating time periods when water levels met or exceeded the level of the ground surface, as established by Auerbach et al. (2015a) in the EGM96 datum. Other locations (RSET-I2 and RSET-S2) were excluded from hydroperiod analysis due to: (i) short time periods of deployment, and (ii) missing or compromised data from instrument vandalism.

3.5. Statistical analyses and parameter comparisons

To evaluate whether seasonal conditions (e.g., monsoonal flooding) significantly impacted surface elevation change and sediment accretion, we compared seasonal changes in these parameters using two-tailed *t*-tests assuming equal variances. In addition, relationships between: (1) hydroperiod and sediment accretion; (2) groundwater level and surface elevation change; and (3) groundwater level and shallow subsidence were assessed for significance using regression analysis. In all cases, a significance level of $\alpha = 0.05$ was used to reject the null hypothesis. Linear trends of surface elevation change were directly compared to local rates of relative sea-level rise (0.9 cm yr^{-1}) to assess whether the investigated landscapes are keeping pace with sea-level change. Relative sea-level rise combines the effects of eustatic sea-level rise at the northern Bay of Bengal (0.3 cm yr^{-1}, Cazenave et al., 2008) and total subsidence (i.e., shallow and deep components, 0.6 cm yr^{-1}, Khan and Islam, 2008; Hanebuth et al., 2013; Grall et al., 2018). No statistical methods were applied to these comparisons as rates of surface elevation change must simply meet or exceed those of sea-level rise to be considered sustainable (e.g., Morris et al., 2002).

4. Results

4.1. Surface elevation change

Among the two hydro-geomorphic settings, the highest rates of surface elevation change were observed at stream-bank sites, where elevation increased over time at a rate of 2.16 ± 0.26 cm yr^{-1} (Fig. 3A; Table 1) and greatly exceeded the rate of relative sea-level rise (0.9 cm yr^{-1}). Surface elevation increased at these locations during both the monsoon and dry season, though positive elevation increments were significantly higher during the monsoon season (Fig. 3A; Table 2). Sundarbans interior sites displayed a slightly lower rate of surface elevation gain, collectively increasing at a rate of 1.32 ± 0.17 cm yr^{-1} (Fig. 3A; Table 1), which also exceeded the rate of relative sea-level rise (0.9 cm yr^{-1}). A strong seasonal signal was apparent in this hydro-geomorphic zone: surface elevation change was positive during the monsoon season but often negative during the dry season (Fig. 3A; Table 2). Over time, however, elevation gain during the monsoon season exceeded elevation loss during the dry season, resulting in an overall positive trend (Fig. 3A).

4.2. Vertical accretion

Rates of vertical accretion as determined by the sediment tile method varied considerably depending on the hydro-geomorphic setting (Fig. 3B). For instance, accretion rates at stream-bank sites (3.29 ± 0.24 cm yr^{-1}) were approximately 55% higher than those at interior sites (2.12 ± 0.20 cm yr^{-1}) (Table 1). This discrepancy was almost exclusively derived from differences in monsoon season accretion as dry season accretion was similar at stream-bank (1.00 ± 0.27 cm) and interior (0.91 ± 0.26 cm) settings (Table 2). Seasonal differences in vertical accretion were significant at Sundarbans stream-bank settings, but not at Sundarbans interior locations (Table 2). Rates of vertical accretion as measured by the marker horizon method were generally higher than those measured by sediment tiles (Table 1). However the horizons, differentiated by color, were often found out of sequence in the subsurface, indicating error associated with bioturbation.

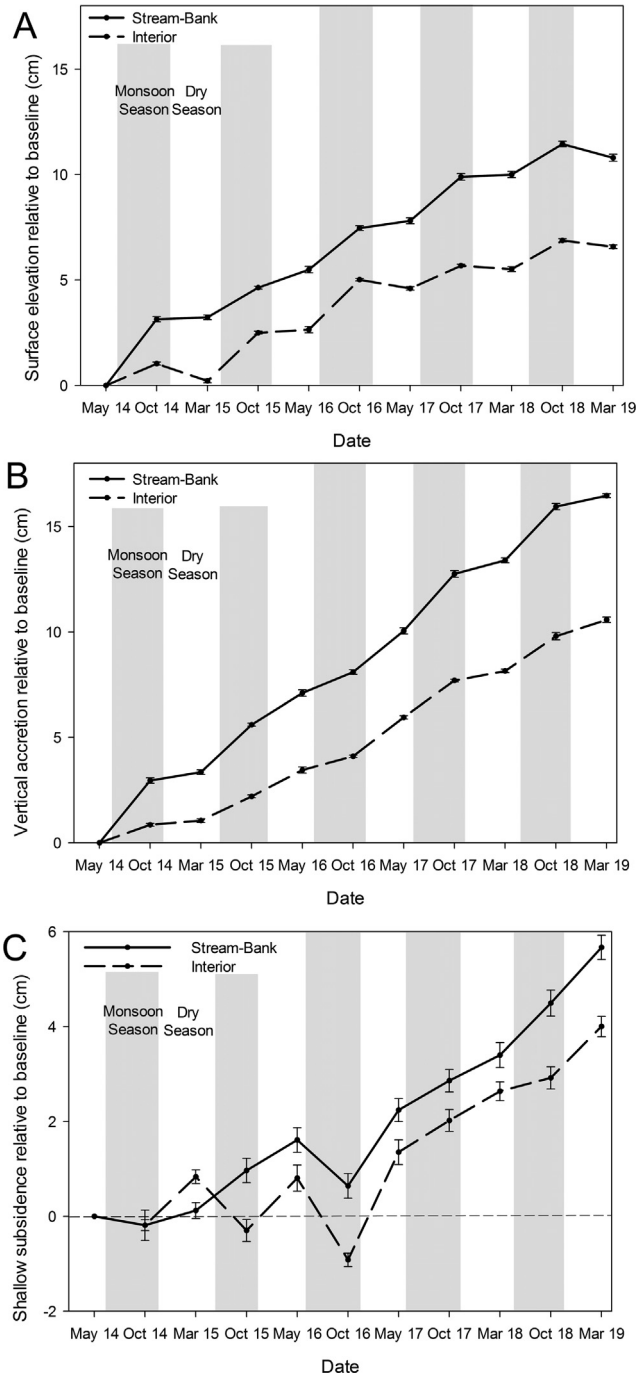

Fig. 3. Inter-annual change in (A) surface elevation, (B) vertical accretion, and (C) shallow subsidence grouped by hydro-geomorphic setting. Note the change in scale for (C) and that values of negative shallow subsidence represent expansion in the shallow subsurface (i.e., clay expansion, belowground biomass production, etc.). Values are the average of two sites and represent longitudinal change relative to the baseline measurement. Error bars are the standard error for all measurements.

4.3. Shallow subsidence

Over the entire dataset, vertical accretion exceeded surface elevation gain at both stream-bank and interior settings, indicating that shallow subsidence occurred between the ground surface and RSET benchmark (Fig. 3C; Table 1). Rates of shallow subsidence at stream-

Table 2
Mean seasonal values (± standard error) of surface elevation change (SEC), vertical accretion using sediment tiles (VA-ST), and shallow subsidence (SS) for the two hydro-geomorphic settings. The presence or absence of significant seasonal differences for the various parameters was established using independent two-tailed *t*-tests (see methods Section 3.5 for more details).

Landscape	Monsoon Season SEC (cm)	Dry Season SEC (cm)	Seasonal Difference in SEC?	Monsoon Season VA (cm)	Dry Season VA (cm)	Seasonal Difference in VA-ST?	Monsoon Season SS (cm)	Dry Season SS (cm)	Seasonal Difference in SS?
Stream-bank	2.01 ± 0.28	0.15 ± 0.22	Yes (t-ratio = 4.69, P = 0.0016)	2.29 ± 0.31	1.00 ± 0.27	Yes (t-ratio = 2.80, P = 0.0231)	0.28 ± 0.34	0.85 ± 0.21	No (t-ratio = 1.29, P > 0.05)
Interior	1.63 ± 0.26	−0.31 ± 0.14	Yes (t-ratio = 5.84, P = 0.0004)	1.21 ± 0.19	0.91 ± 0.26	No (t-ratio = 0.83, P > 0.05)	−0.42 ± 0.40	1.22 ± 0.25	Yes (t-ratio = 3.13, P = 0.0141)

bank sites (1.13 ± 0.50 cm yr^{-1}) were ~34% higher than those of interior sites (0.80 ± 0.37 cm yr^{-1}, Table 1). Seasonal patterns of shallow subsidence were similar for both hydro-geomorphic settings, exhibiting greater subsidence during the dry season than during the monsoon season (Fig. 3C). There were, however, a couple instances during the monsoon season when surface elevation gain exceeded vertical accretion, indicating shallow subsurface expansion (e.g., between May and October 2016, Fig. 3C).

4.4. Platform flooding

Surface hydrologic data recorded within the tidal channel at Suterkhali dock (see Fig. 1B for location) reveal that the local area is characterized by a semidiurnal tidal regime with a tide range of ~3 to 5 m (Fig. 4A). A water level setup of ~0.5 to 0.7 m is observed during the monsoon season (Fig. 4A), as documented in other coastal regions of the G-B delta (Barua, 1990). GPS and theodolite surveys undertaken by Auerbach et al. (2015a) determined the average elevation of the Sundarbans relative to pertinent tidal frame constituents, including mean high water (MHW), mean sea level (MSL), and mean low water (MLW), within the EGM96 datum (Fig. 4A). Comparing the average elevation of the Sundarbans, +2.6 m relative to EGM96, to the Suterkhali tide data suggests that during the monsoon season, flooding of the mangrove platform should occur during every spring high tide up to ~0.5 m depth and during a few isolated neap high tides (Fig. 4A). This approach also suggests that platform inundation during the dry season should occur during new moon spring tides, with little flooding otherwise (Fig. 4A).

The hydrodynamics from piezometers located on the Sundarbans mangrove platform display weekly, large-scale fluctuations in water level due to neap-spring tidal cycles (Fig. 4B). When placed within the context of the mangrove platform ground surface, this data indicates when the platform is inundated and the depth of inundation, as well as the shallow groundwater table dynamics (Fig. 4B, C). Piezometer results generally substantiate tide gauge approximations of inundation and indicate that during the monsoon season platform inundation occurs during the majority of spring high tides and occasionally during neap high tides (Fig. 4B). In contrast, platform flooding during the dry season is relatively scarce, occurring only during some new moon spring tides and exhibiting evidence of negligible inundation for several weeks to months at a time (e.g., between Dec 16 and Feb 17, Fig. 4B, C). Shallow groundwater table dynamics are controlled by neap-spring cyclicity and seasonal conditions (Fig. 4B). During the monsoon season, the groundwater table typically lowers 0.3–0.5 m relative to the platform surface (Fig. 4B). Groundwater fluctuations are more dramatic during the dry season, when lowering of the groundwater table in excess of 1 m was documented on multiple occasions (e.g., between Jan and Feb 17, Fig. 4B). Over the cumulative dataset, stream-bank site RSET-S1 documented greater hydroperiod in comparison to interior site RSET-I1, though there were multiple months when the hydroperiod of RSET-I1 exceeded that of RSET-S1 (e.g., Nov 15, Fig. 4C).

5. Discussion

5.1. Surface controls on landscape dynamics

Rates of surface elevation change and sediment accretion from this study, which represent the first coordinated measurements in the G-B tidal delta plain, were in general much greater than those reported in other mangrove systems. In a review of mangrove settings across the worldwide RSET network, Sasmito et al. (2016) found that for pristine mangrove sites with > 1 year of data (n = 45), surface elevation and vertical accretion rates averaged 0.07 and 0.55 cm yr^{-1}, respectively. Corresponding measurements from this study, averaging 1.74 and 2.71 cm yr^{-1} for our study sites in the natural Sundarbans mangrove forest (Table 1), are up to an order of magnitude greater than the

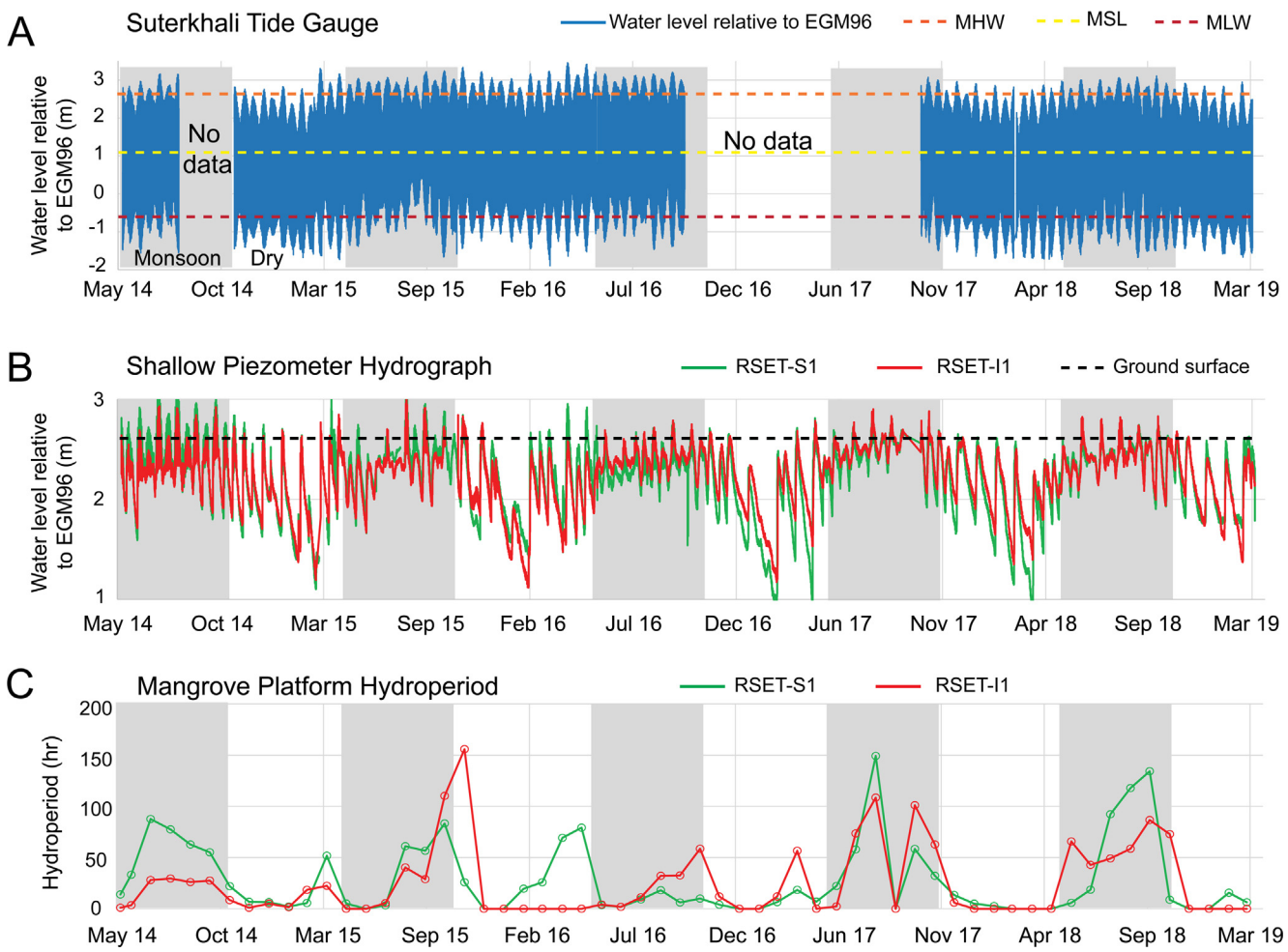

Fig. 4. (A) Water level measurements at Suterkhali dock (see Fig. 1B) including local tidal frame constituents. Note that during the monsoon season (time periods shaded in grey) there is a coastal set-up of water regionally (after Barua, 1990), which raises mean water level by ~50–70 cm. Abbreviations: MHW- mean high water; MSL - mean sea level; MLW - mean low water (after Auerbach et al., 2015a). (B) Hydrographs for shallow piezometers near RSET-S1 and RSET-I1, located within the Sundarbans (see Fig. 1B), illustrating fluctuations in water level related to neap-spring cycles during the dry (white) and monsoon (grey) seasons. The dashed line represents the overbank flooding threshold (i.e., mangrove platform elevation), which is only surpassed ~every 2 weeks during the monsoon season spring tides. Note that during neap tides, groundwater levels lower as much as ~1.25 m, exacerbated during the dry season when the platform hydroperiod is reduced by ~62% (see also Fig. 5). (C) Monthly tidal hydroperiod of the mangrove platform at RSET-S1 and RSET-I1 locations.

worldwide average, which underscores the amount of sediment discharged from the G-B river mouth, as well as the efficiency of the system to redistribute these sediments to the tidal delta plain (~150–200 km from the river mouth, *sensu* Rogers et al., 2013; Wilson and Goodbred, 2015). To our knowledge, the only location with comparably high rates of surface elevation change is at Sanjiang in Dongzhaiguang Bay, China, where elevation increased at an average rate of 1.75 cm yr^{-1} (Fu et al., 2018). The mangrove forests of the Sundarbans and Sanjiang share commonality as mineral-rich, riverine systems that are situated in the vicinity of large population centers (Rogers et al., 2013; Fu et al., 2018). Owing to a general lack of organic matter accumulation in this type of environment (e.g., Rovai et al., 2018), mineral-rich, riverine mangrove systems are heavily reliant on the continued supply of upstream sediments in order to maintain positive surface elevation change over time.

Vertical accretion measurements using the marker horizon method in this study generally yielded higher values than analogous measurements using sediment tiles (Table 1). Based on the observation that marker horizons were often found out of sequence in the subsurface, we attribute this difference to the presence of post-depositional mixing (i.e., bioturbation). Mangrove crabs (*Scylla serrata*) are abundant in the Sundarbans forest and commonly burrow during low tide (Alberts-Hubatsch et al., 2016), likely altering the subsurface particle distribution. On the other hand, sediment tiles provide a physical barrier that prevents mixing of older sediments, likely yielding more accurate vertical accretion and shallow subsidence rates (Table 1). Nevertheless, the sediment accretion rates derived from both techniques in this study may be overestimated as short-term additive measurements typically yield higher values than a single long-term measurement that incorporates sediment dewatering and compaction (e.g., Steiger et al., 2003). Therefore, the rates of shallow subsidence reported here (Fig. 3C, Table 1) should be viewed as upper estimates for this region. Additionally, we acknowledge that due to the relatively short duration of this study (5 years), our rates of sediment accretion will naturally be higher than those obtained using techniques that investigate longer time scales (e.g., decadal to centennial sedimentation rates from short-lived radioisotopes, e.g., Allison and Kepple, 2001) because of compaction and differences in the time scales involved (Sadler, 1981), and thus should not be directly compared.

In the G-B tidal delta plain, we find that the patterns of surface elevation change reflect hydrodynamic processes that are in turn governed by seasonal climatic conditions. During the summer monsoon, elevated suspended sediment concentrations in the tidal channels (Barua, 1990; Hale et al., 2019a; Hale et al., 2019b) combined with

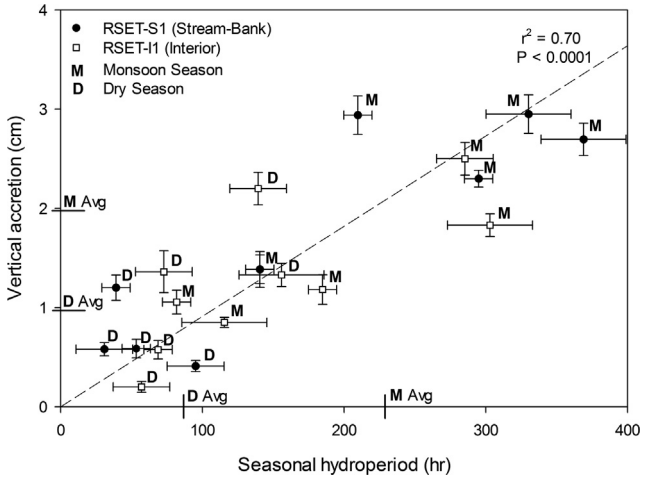

Fig. 5. Relationship between observed vertical accretion on tiles and calculated seasonal inundation for RSET-S1 and RSET-I1 locations in the Sundarbans mangrove forest.

increased frequency of platform inundation (from an average of 85.2 ± 42.9 h to 229.2 ± 95.9 h; Figs. 4C, 5) promote surface elevation gain, principally through the accumulation of newly deposited sediment (*sensu* Marion et al., 2009). Indeed, we found that the duration of inundation of the platform (i.e., hydroperiod) strongly controls the magnitude of sediment accretion as presented earlier: a significant positive relationship exists between these two parameters ($r^2 = 0.70$, $P < 0.0001$; Fig. 5). Accordingly, elevation gains were significantly greater during the monsoon season as compared to during the dry season at all hydro-geomorphic settings (Table 2). We note however, similar to other wetland settings, seasonal differences in sediment accretion were site-specific (Table 2). Sundarbans stream-bank locations exhibited seasonal differences in accretion, likely reflecting greater access to the sediment-rich waters of the monsoon season (Hale et al., 2019a). On the other hand, Sundarbans interior sites did not exhibit seasonal differences in sediment accretion, suggesting that part of the monsoon sediment load was sequestered on or near the channel banks and did not reach the interior of the mangrove platform (*sensu* Rogers and Goodbred, 2014).

Mangrove vegetation density likely also plays a role in the capture and deposition of sediments carried in suspension by tidal waters. Hydrodynamic field and modeling studies in a number of mangrove forests indicate that the interaction between tidal currents and subaerial vegetation (e.g., pneumatophores) produces zones of stagnant water in which suspended sediments preferentially settle (Furukawa and Wolanski, 1996; Furukawa et al., 1997; Krauss et al., 2003; Anthony, 2004; Van Santen et al., 2007). Correspondingly, it is possible that a portion of the total sediment load carried by flood tides is deposited within close proximity of the channel, effectively diluting the tidal water as it propagates towards the interior of the platform (e.g., Furukawa and Wolanski, 1996). Hale et al. (2019b) documented a 15% reduction in peak suspended sediment concentration from stream-bank (RSET-S2 in this study) to interior sites (RSET-I2 in this study) in the monsoon season, corroborating the notion of progressive sediment extraction from tidal waters. Generally higher than expected rates of sediment accretion at Sundarbans sites during the dry season could be attributed to the facilitated deposition of silt- and clay-size particles via electrochemical flocculation (e.g., Winterwerp and van Kesteren, 2004) when waters are relatively saline during this time of the year (up to 25 ppt, Shaha and Cho, 2016). Silt and clay are the dominant grain sizes in the Sundarbans mangrove forest, together accounting for > 85% of the near-surface sediments (depth = 10–50 cm) in the study area (Allison et al., 2003).

5.2. Subsurface controls on landscape dynamics

It is well established that vertical accretion is a strong influence on surface elevation change in wetlands and deltaic settings (e.g., Nyman et al., 2006; Neubauer, 2008), however it is not the only parameter that controls displacement of the land surface through time. As seen by differences in surface elevation and vertical accretion (cf. Fig. 3A and B; Table 1), a portion of the absolute elevation gain can be lost to below-ground processes and resultant shallow subsidence. In general, a variety of subsurface processes in wetlands contribute to shallow subsidence, including groundwater flux (Cahoon et al., 1995; Whelan et al., 2005, Rogers and Saintilan, 2008), sediment compaction (Knott et al., 1987; Day et al., 1999; Lovelock et al., 2011), clay abundance and mineralogy (Schafer and Singer, 1976; Karathanasis and Hajek, 1985; Nelson and Miller, 1992), and organic matter production and decomposition (Cahoon et al., 2003; McKee et al., 2007). These studies show that the relative importance of these factors is highly location-specific; therefore, careful consideration of each of these processes is critical when characterizing landscape evolution.

The presence of both subsidence and expansion of the substrate in this study area using RSET methods (Fig. 3C) coupled with groundwater piezometer data (Fig. 4B) suggest that seasonal fluctuations in shallow groundwater level (< 2 m depth) influence landscape dynamics in the natural G-B tidal delta plain. This is demonstrated through a positive and significant relationship between deviations in groundwater level and surface elevation change ($r^2 = 0.76$, $P < 0.0001$; Fig. 6A).

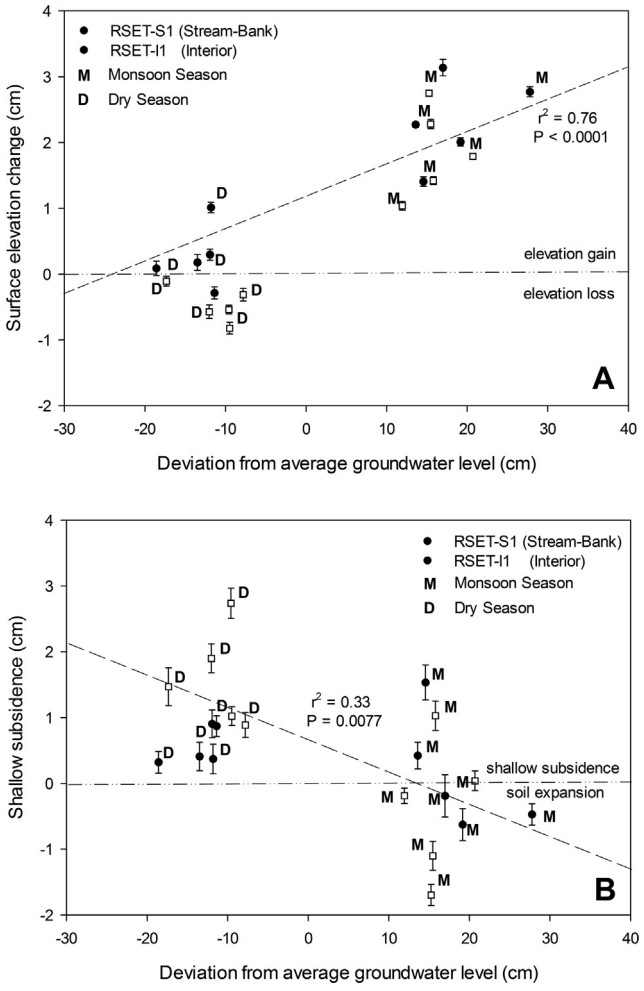

Fig. 6. Seasonal relationships between (A) surface elevation change and (B) shallow subsidence with normalized differences in groundwater level from RSET and piezometers located within the Sundarbans mangrove forest.

Similarly, a negative and significant relationship is observed between deviations in groundwater level and shallow subsidence and expansion (r^2 = 0.33, P = 0.0077; Fig. 6B). These seasonal relationships among groundwater level, surface elevation change, and shallow subsidence suggest that more frequent flooding during the monsoon promotes groundwater recharge and soil swelling (e.g., Harvey et al., 2006), contributing to surface elevation gain (Fig. 6A) and substrate expansion (Fig. 6B). Conversely, less frequent flooding coupled with enhanced evapotranspiration rates during the dry season (e.g., Brammer, 2004) leads to soil desiccation, shallow subsidence (Figs. 3C, 6B), and surface elevation loss (Fig. 6A). The swelling and shrinking of near-surface sediments in response to volumetric changes in pore-water is a well-documented phenomenon (e.g., Nuttle and Hemand, 1988; Nuttle et al., 1990; Whelan et al., 2005) that has been reported in other locations with seasonal climates. For instance, work in the mangrove forests of Everglades National Park, Florida, USA demonstrated that monthly changes in surface elevation were strongly correlated with coincident variations in groundwater level (Whelan et al., 2005).

It is also well recognized that clay mineralogy is a primary control on the shrink and swell potential of sediments and soils (e.g., Schafer and Singer, 1976; Karathanasis and Hajek, 1985). Sediments in southwest Bangladesh contain a clay mineral assemblage that is primarily composed of illite (~60%), with lesser amounts of smectite, chlorite, and kaolinite (~10–15% each, Allison et al., 2003). Among clay mineral suites, those with high illite and minor smectite components have a "moderate to high" shrink and swell potential (Nelson and Miller, 1992), which along with lowering of the groundwater table documented here (Figs. 4B, 6), may explain the pronounced seasonal differences of elevation change and sediment accretion within the Sundarbans (Fig. 3A, B, Table 2).

Previous laboratory and field studies in coastal settings suggest that substrate compaction is strongly controlled by sediment organic content, wherein organic-rich sediments like peat are more compressible and prone to compaction than inorganic sediments like detrital sand and silt (e.g., Knott et al., 1987; van Asselen et al., 2009). The surface sediments (i.e., 0–2 cm depth) of the Sundarbans mangrove forest are very low in organic content, ranging between 2.9 and 3.8% by mass (Rogers et al., 2013), and this trend continues to > 1 m depth (Allison et al., 2003; Bomer et al., 2019). Based on these observations it follows that organic compaction should not compose a large proportion of the shallow subsidence. We thus postulate that in the case of the mineral-rich G-B tidal delta plain, bulk grain size and water and clay content of the shallow stratigraphy are more likely to control the magnitude of compaction. We also note it is likely that compaction-induced subsidence also occurs below the RSET benchmark where overburden pressure is greater (i.e., "deep subsidence," Cahoon et al., 1995), however, due to the depth limitations of RSET investigations, the relative contribution of deep subsidence is not quantified here (requires other methods such as GPS or stratigraphic age control, see Steckler et al., 2010; Grall et al., 2018). Recent geodetic reports have provided insights on total subsidence (i.e., shallow plus deep components) in the eastern part of the G-B delta, demonstrating that rates of total subsidence range from 0 to 1.8 cm yr^{-1} (Higgins et al., 2014). In this study, rates of shallow subsidence across all locations ranged from 0.70 to 1.84 cm yr^{-1} (Table 1), which when compared to the rates of total subsidence from Higgins et al. (2014), suggests that the majority of compaction in this delta occurs in the uppermost ~10 to 20 m of the subsurface. This notion is consistent with the findings of Törnqvist et al. (2008), who show that in the Mississippi River Delta much of the subsidence results from the compaction of relatively shallow (~15 m depth), Holocene-age sediments.

5.3. Sea-level rise and landscape vulnerability

The long-term sustainability of mangrove forests and other low-lying coastal landscapes requires that gains in surface elevation must meet or exceed rates of sea-level rise (e.g., Woodroffe et al., 2016). Our data indicate that the natural G-B tidal delta plain is much less vulnerable to sea level-induced submergence than previously thought (e.g., Houghton, 2005; Loucks et al., 2010). We document that surface elevation gain at stream-bank (2.16 ± 0.26 cm yr^{-1}) *and* interior sites (1.32 ± 0.17 cm yr^{-1}) in the Sundarbans greatly outpaces the rate of relative sea-level rise (0.9 cm yr^{-1}) (Fig. 7). Furthermore, it seems apparent that relative sea-level rise plus the effects of tidal amplification (which combined = 1.2–1.6 cm yr^{-1}, hereafter referred to as "effective sea-level rise," *sensu* Pethick and Orford, 2013) is a more dominant control on the mangrove surface geomorphic evolution. The results of this study indicate that the surface elevation of the Sundarbans mangrove platform (both stream-bank and interior settings) is increasing in response to changes in the level of mean high water (MHW) instead of eustatic sea-level rise (Fig. 7). This finding highlights the adaptability of mangrove ecosystems to local environmental disturbances (e.g., Alongi, 2008), in this case to tidal amplification and associated increase in platform flooding from embankment-induced channel constriction (Pethick and Orford, 2013). This adaptability mechanism is reflected in the geomorphic stability of the Sundarbans mangrove forest. For instance, remote sensing research across the Sundarbans indicates little conversion of interior mangrove platforms to open water over the past 30 years (Giri et al., 2007), most likely a result of effective sediment distribution through the interior of the tidal delta plain by smaller-order tidal creeks (Rogers et al., 2013; Hale et al., 2019b). These large-scale observations, along with findings from the present study, contradict oversimplified models of land loss which put forth the notion that low elevation areas, such as the Sundarbans interior sites, passively submerge in response to rising sea levels (Houghton, 2005; Loucks et al., 2010).

Although the proceedings of this study represent an important first step in quantifying elevation and sedimentation dynamics in the Sundarbans and G-B tidal delta plain, we acknowledge that our results may not be representative of the entire Sundarbans mangrove forest. For example, changes in surface elevation near the Bay of Bengal may be less influenced by tidal amplification (quantified as 0.3 cm yr^{-1} in this area by Pethick and Orford, 2013) and more influenced by higher subsidence rates as a result of thicker sediment loading (quantified as 0.5 cm yr^{-1} in this area by Grall et al., 2018). Similarly, the western portion of the Sundarbans forest likely experiences less deposition as a

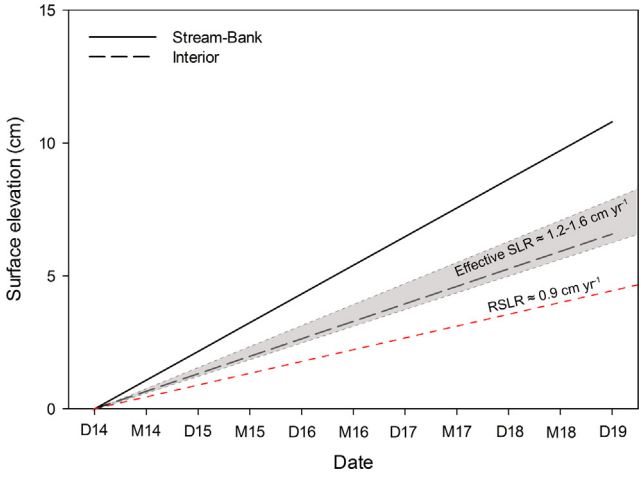

Fig. 7. Linear trajectories for surface elevation change at hydro-geomorphic settings compared to upper and lower estimates of sea-level rise: relative sea-level rise (RSLR) integrates the effects of eustatic sea-level rise and subsidence (Cazenave et al., 2008; Khan and Islam, 2008; Hanebuth et al., 2013; Grall et al., 2018) whereas effective sea-level rise includes the effects of RSLR plus tidal range amplification from embankment construction (Pethick and Orford, 2013). "D" and "M" refer to dry and monsoon seasons while the numbers correspond to the year (e.g., D14 = dry season of 2014).

result of the increased distance from the G-B river mouth (Flood et al., 2018). Differences in elevation and sedimentation dynamics between the Sundarbans and human-impacted regions of the G-B tidal delta plain are likely to be even more pronounced due to extensive anthropogenic modification of the landscape and tidal channel network (Auerbach et al., 2015a; Wilson et al., 2017). We hypothesize that such landscapes are not adapting sufficiently to changes in sea-level rise based on reports of polders being situated ~1 m below mean high water (Auerbach et al., 2015a). However, we stress that further research is necessary to constrain the spectrum of these parameters, and the resulting geomorphic expression, across the greater G-B tidal delta plain.

Although natural, unmodified areas of the G-B delta appear to be currently sustainable as presented here, major concerns for the long-term future of the delta are still present, particularly with respect to reductions in sediment supply from upstream sources. Over the next 30 years, India's National River Linking Project is expected to add 43 dams and 29 link canals to the country's infrastructure, leading to substantial downstream reductions in suspended sediment load for the Ganges and Brahmaputra rivers, estimated at 39–75% and 9–25%, respectively (Higgins et al., 2018). If such upstream blockages and associated reductions in sediment load are realized, aggradation rates would decrease delta-wide (Higgins et al., 2018), weakening the natural defense of the system to relative and effective sea-level rise, and ultimately render the G-B delta more vulnerable to the effects of global climate change. Finally, it should be stressed that in the G-B tidal delta plain and possibly other coastal systems, *effective sea-level rise* is the main hydrodynamic parameter that places human livelihood at risk, given that the land surface relative to MHW is ultimately what dictates flood risk and associated damage to crops and infrastructure. Future studies should consider the range of anthropogenic practices involved and constrain the magnitude of their influence on depositional conditions to properly evaluate landscape evolution.

6. Conclusions

In the G-B tidal delta plain, surface elevation change is controlled by a variety of factors that occur both at the surface (e.g., sediment deposition, tidal flooding) and in the shallow subsurface (e.g., seasonal groundwater fluctuations, hydro-expansion and contraction of clay minerals, sediment compaction). Newly available inter-annual records of surface elevation, vertical accretion, and shallow subsidence in the G-B tidal delta plain reveal much needed insights on the sustainability of this region. In this study, we document that in the natural streambank and interior settings of the Sundarbans mangrove forest, which remain hydrologically connected to sediment-laden tidal waters, elevation gain is occurring at rates of $2.16 \pm 0.26\,cm\,yr^{-1}$ and $1.32 \pm 0.17\,cm\,yr^{-1}$, respectively. These rates of elevation gain exceed that of relative sea-level rise ($0.9\,cm\,yr^{-1}$) and more closely follow the range of effective sea-level rise ($1.2–1.6\,cm\,yr^{-1}$, Pethick and Orford 2013), suggesting that the natural land surface is maintaining equilibrium with changes in mean high water. Overall, the findings of this research highlight the adaptability and responsiveness of the natural G-B tidal delta plain to maintain positive surface elevation in the face of locally accelerated sea-level rise. However, the long-term fate of the delta hinges upon the continued supply of sediments from upstream source areas. Future infrastructure projects that re-route water and sediment conveyance pathways away from the lower G-B delta increases the vulnerability of this low-lying coastal region to sea-level rise and submergence.

Acknowledgments

This study was funded by Office of Naval Research grant #N00014-11-1-0683, National Science Foundation Belmont Forum grant #1342946, and National Science Foundation Coastal SEES grant #1600258. Much gratitude is extended to the following individuals for their assistance with field and lab work: Abdullah Al Nahian, Sourov Bijoy Datta, Cameron Gernant, Md. Saddam Hossian, Nithy Khair, and Matthew Winters. Special thanks to Md. Nazrul "Bachchu" Islam and Pugmark Tours for handling logistics throughout numerous field campaigns.

Author contributions

CW developed the study concept, obtained funding, and established the methods. EB, CW, RH, AH, and AR carried out field work. The first manuscript draft was written by EB and revised by all co-authors. All authors contributed to the intellectual content expressed herein.

Declaration of Competing Interest

The authors declared that there is no conflict of interest.

Appendix A. Supplementary material

Supplementary data to this article can be found online at https://doi.org/10.1016/j.catena.2019.104312.

References

Alam, M., 1996. Subsidence of the Ganges—Brahmaputra Delta of Bangladesh and associated drainage, sedimentation and salinity problems. In: Sea-Level Rise and Coastal Subsidence. Springer, Dordrecht, pp. 169–192.

Alberts-Hubatsch, H., Lee, S.Y., Meynecke, J.O., Diele, K., Nordhaus, I., Wolff, M., 2016. Life-history, movement, and habitat use of Scylla serrata (Decapoda, Portunidae): current knowledge and future challenges. Hydrobiologia 763, 5–21. https://doi.org/10.1007/s10750-015-2393-z.

Allison, M.A., 1998. Geologic framework and environmental status of the Ganges-Brahmaputra Delta. J. Coast. Res. 14, 827–836.

Allison, M., Kepple, E., 2001. Modern sediment supply to the lower delta plain of the Ganges-Brahmaputra River in Bangladesh. Geo-Mar. Lett. 21, 66–74. https://doi.org/10.1007/s003670100069.

Allison, M.A., Khan, S.R., Goodbred, S.L., Kuehl, S.A., 2003. Stratigraphic evolution of the late Holocene Ganges-Brahmaputra lower delta plain. Sed. Geol. 155, 317–342. https://doi.org/10.1016/S0037-0738(02)00185-9.

Alongi, D.M., 2008. Mangrove forests: resilience, protection from tsunamis, and responses to global climate change. Estuar. Coast. Shelf Sci. 76, 1–13. https://doi.org/10.1016/j.ecss.2007.08.024.

Anthony, E.J., 2004. Sediment dynamics and morphological stability of an estuarine mangrove complex: Sherbro Bay, West Africa. Mar. Geol. 208, 207–224. https://doi.org/10.1016/j.margeo.2004.04.009.

Auerbach, L.W., Goodbred, S.L., Mondal, D.R., Wilson, C.A., Ahmed, K.R., Roy, K., et al., 2015a. Flood risk of natural and embanked landscapes on the Ganges-Brahmaputra tidal delta plain. Nat. Clim. Change 5, 153–157. https://doi.org/10.1038/nclimate2472.

Auerbach, L.W., Goodbred, S.L., Mondal, D.R., Wilson, C.A., Ahmed, K.R., Roy, K., et al., 2015b. Reply to 'Tidal river management in Bangladesh'. Nat. Clim. Change 5, 492. https://doi.org/10.1038/nclimate2472.

Barua, D.K., 1990. Suspended sediment movement in the estuary of the Ganges-Brahmaputra-Meghna river system. Mar. Geol. 91, 243–253. https://doi.org/10.1016/0025-3227(90)90039-M.

Barua, D.K., Kuehl, S.A., Miller, R.L., Moore, W.S., 1994. Suspended sediment distribution and residual transport in the coastal ocean off the Ganges-Brahmaputra river mouth. Mar. Geol. 120, 41–61. https://doi.org/10.1016/0025-3227(94)90076-0.

BIWTA (Bangladesh Inland Water Transport Authority), 2019. Bangladesh Tide Tables, 2019. Department of Hydrography, Dhaka, Bangladesh.

Bomer, E.J., Wilson, C.A., Quirk, T., 2019. Belowground controls on surface elevation change and carbon sequestration potential of the Sundarbans Mangrove Forest, Bangladesh. Society of Wetland Scientists Annual Meeting 2019, Abstract ID #1259.

Brammer, H., 2004. Can Bangladesh be Protected from Floods? University Press Limited, Dhaka.

Cahoon, D.R., 2015. Estimating relative sea-level rise and submergence potential at a coastal wetland. Estuar. Coasts 38, 1077–1084. https://doi.org/10.1007/s12237-014-9872-8.

Cahoon, D.R., Turner, R.E., 1989. Accretion and canal impacts in a rapidly subsiding wetland II: feldspar marker horizon technique. Estuaries 12, 260–268. https://doi.org/10.2307/1351905.

Cahoon, D.R., Reed, D.J., Day, J.W., 1995. Estimating shallow subsidence in microtidal salt marshes of the southeastern United States: Kaye and Barghoorn revisited. Mar. Geol. 128, 1–9. https://doi.org/10.1016/0025-3227(95)00087-F.

Cahoon, D., Hensel, P., Rybczyk, J., McKee, K., Proffitt, C., Perez, B., 2003. Mass tree mortality leads to mangrove peat collapse at Bay Islands, Honduras after Hurricane Mitch. J. Ecol. 91 (6), 1093–1105.

Cahoon, D.R., Lynch, J.C., Perez, B.C., Segura, B., Holland, R.D., Stelly, C., et al., 2002.

High-precision measurements of wetland sediment elevation: II. The rod surface elevation table. J. Sediment. Res. 72, 734–739. https://doi.org/10.1306/020702720734.
Cahoon, D.R., Hensel, P.F., 2006. High-resolution global assessment of mangrove response to sea-level rise: a review. In: Proceedings of the Symposium on Mangrove Responses to Relative Sea-Level Rise and Other Climate Change Effects, pp. 9–17.
Cazenave, A., Lombard, A., Llovel, W., 2008. Present-day sea level rise: a synthesis. C.R. Geosci. 340, 761–770. https://doi.org/10.1016/j.crte.2008.07.008.
Church, J.A., White, N.J., 2006. A 20th century acceleration in global sea-level rise. Geophys. Res. Lett. 33, 1–4. https://doi.org/10.1029/2005GL024826.
Coleman, J.M., 1969. Brahmaputra River: channel processes and sedimentation. Sed. Geol. 3, 129–239. https://doi.org/10.1016/0037-0738(69)90010-4.
Day, J.W., Rybczyk, J., Scarton, F., Rismondo, A., Are, D., Cecconi, G., 1999. Soil accretionary dynamics, sea-level rise and the survival of wetlands in Venice Lagoon: a field and modelling approach. Estuar. Coast. Shelf Sci. 49, 607–628. https://doi.org/10.1006/ecss.1999.0522.
EGIS – (Environmental and Geographical Information System), 2000. Environmental Baseline of Gorai River Restoration Project, EGIS-II. Bangladesh Water Development Board, Ministry of Water Resources, Government of Bangladesh, Delft, the Netherlands, pp. 150.
Flood, R.P., Barr, I.D., Weltje, G.J., Roberson, S., Russell, M.I., Meneely, J., Orford, J.D., 2018. Provenance and depositional variability of the thin mud facies in the lower Ganges-Brahmaputra delta, West Bengal Sundarbans, India. Mar. Geol. 395, 198–218.
Fu, H., Wang, W., Ma, W., Wang, M., 2018. Differential in surface elevation change across mangrove forests in the intertidal zone. Estuar. Coast. Shelf Sci. 207, 203–208. https://doi.org/10.1016/j.ecss.2018.03.025.
Furukawa, K., Wolanski, E., 1996. Sedimentation in mangrove forests. Mangr. Salt Marsh. 1, 3–10.
Furukawa, K., Wolanski, E., Mueller, H., 1997. Currents and sediment transport in mangrove forests. Estuar. Coast. Shelf Sci. 44, 301–310. https://doi.org/10.1006/ecss.1996.0120.
Giri, C., Pengra, B., Zhu, Z., Singh, A., Tieszen, L.L., 2007. Monitoring mangrove forest dynamics of the Sundarbans in Bangladesh and India using multi-temporal satellite data from 1973 to 2000. Estuar. Coast. Shelf Sci. 73, 91–100. https://doi.org/10.1016/j.ecss.2006.12.019.
Giri, S., Mukhopadhyay, A., Hazra, S., Mukherjee, S., Roy, D., Ghosh, S., et al., 2014. A study on abundance and distribution of mangrove species in Indian Sundarban using remote sensing technique. J. Coast. Conserv. 18, 359–367. https://doi.org/10.1007/s11852-014-0322-3.
Grall, C., Steckler, M.S., Pickering, J.L., Goodbred, S., Sincavage, R., Paola, C., Akhter, S.H., Spiess, V., 2018. A base-level stratigraphic approach to determining Holocene subsidence of the Ganges–Meghna–Brahmaputra Delta plain. Earth Planet. Sci. Lett. 499, 23–36. https://doi.org/10.1016/j.epsl.2018.07.008.
Hale, R.P., Bain, R., Goodbred Jr., S., Best, J., 2019a. Observations and scaling of tidal mass transport across the lower Ganges-Brahmaputra delta plain: implications for delta management and sustainability. Earth Surf. Dyn. 7, 231–245. https://doi.org/10.5194/esurf-2018-66.
Hale, R.P., Wilson, C.A., Bomer, E.J., 2019b. Seasonal variability of forces controlling sedimentation in the Sundarbans National Forest, Bangladesh. Front. Earth Sci. 7, 1–13. https://doi.org/10.3389/feart.2019.00211.
Hanebuth, T., Kudrass, H., Linstädter, J., Islam, B., Zander, A., 2013. Rapid coastal subsidence in the central Ganges-Brahmaputra Delta (Bangladesh) since the 17th century deduced from submerged salt-producing kilns. Geology 41, 987–990.
Harvey, C.F., Ashfaque, K.N., Yu, W., Badruzzaman, A.B.M., Ali, M.A., Oates, P.M., Michael, H.A., Neumann, R.B., Beckie, R., Islam, S., Ahmed, M.F., 2006. Groundwater dynamics and arsenic contamination in Bangladesh. Chem. Geol. 228, 112–136. https://doi.org/10.1016/j.chemgeo.2005.11.025.
Higgins, S.A., Overeem, I., Steckler, M.S., Syvitski, J.P., Seeber, L., Akhter, S.H., 2014. InSAR measurements of compaction and subsidence in the Ganges-Brahmaputra Delta, Bangladesh. J. Geophys. Res. Earth Surf. 119, 1768–1781.
Higgins, S.A., 2016. Review: Advances in delta-subsidence research using satellite methods. Hydrogeol. J. 24, 587–600. https://doi.org/10.1007/s10040-015-1330-6.
Higgins, S.A., Overeem, I., Rogers, K.G., Kalina, E.A., 2018. River linking in India: downstream impacts on water discharge and suspended sediment transport to deltas. Elementa 6, 1–24. https://doi.org/10.1525/elementa.269.
Hossain, F., Khan, Z.H., Shum, C.K., 2015. Tidal river management in Bangladesh. Nat. Clim. Change 5, 492. https://doi.org/10.1038/nclimate2618.
Houghton, J., 2005. Global warming. Rep. Prog. Phys. 68, 1343–1403. https://doi.org/10.1088/0034-4885/68/6/R02.
Islam, M.R., 2006. Managing diverse land uses in coastal Bangladesh. In: Environment and Livelihoods in Tropical Coastal Zones, pp. 237–248.
Jevrejeva, S., Moore, J.C., Grinsted, A., Woodworth, P.L., 2008. Recent global sea level acceleration started over 200 years ago? Geophys. Res. Lett. 35, 1–4. https://doi.org/10.1029/2008GL033611.
Karathanasis, A.D., Hajek, B.F., 1985. Shrink – swell potential of montmorillonitic soils in udic moisture regimes. Soil Sci. Soc. Am. J. 49, 159–166.
Khan, S.R., Islam, B., 2008. Holocene stratigraphy of the lower Ganges-Brahmaputra river delta in Bangladesh. Front. Earth Sci. China 2, 393–399. https://doi.org/10.1007/s11707-008-0051-8.
Kirwan, M.L., Guntenspergen, G.R., 2010. Influence of tidal range on the stability of coastal marshland. J. Geophys. Res. Earth Surf. 115, 1–11. https://doi.org/10.1029/2009JF001400.
Kirwan, M.L., Megonigal, J.P., 2013. Tidal wetland stability in the face of human impacts and sea-level rise. Nature 504, 53–60. https://doi.org/10.1038/nature12856.
Knott, J.F., Nuttle, W.K., Hemond, H.F., 1987. Hydrologic parameters of salt marsh peat. Hydrol. Process. 1, 211–220. https://doi.org/10.1002/hyp.3360010208.
Krauss, K.W., Allen, J.A., Cahoon, D.R., 2003. Differential rates of vertical accretion and elevation change among aerial root types in Micronesian mangrove forests. Estuar. Coast. Shelf Sci. 56, 251–259. https://doi.org/10.1016/S0272-7714(02)00184-1.
Krauss, K.W., Cahoon, D.R., Allen, J.A., Ewel, K.C., Lynch, J.C., Cormier, N., 2010. Surface elevation change and susceptibility of different mangrove zones to sea-level rise on Pacific high islands of Micronesia. Ecosystems 13, 129–143.
Loucks, C., Barber-Meyer, S., Hossain, M.A.A., Barlow, A., Chowdhury, R.M., 2010. Sea level rise and tigers: predicted impacts to Bangladesh's Sundarbans mangroves. Clim. Change 98, 291–298. https://doi.org/10.1007/s10584-009-9761-5.
Lovelock, C.E., Bennion, V., Grinham, A., Cahoon, D.R., 2011. The role of surface and subsurface processes in keeping pace with sea level rise in intertidal wetlands of Moreton Bay, Queensland, Australia. Ecosystems 14, 745–757. https://doi.org/10.1007/s10021-011-9443-9.
Marion, C., Anthony, E.J., Trentesaux, A., 2009. Short-term (≤ 2 yrs) estuarine mudflat and saltmarsh sedimentation: high-resolution data from ultrasonic altimetery, rod surface-elevation table, and filter traps. Estuar. Coast. Shelf Sci. 83, 475–484. https://doi.org/10.1016/j.ecss.2009.03.039.
McKee, K.L., Cahoon, D.R., Feller, I.C., 2007. Caribbean mangroves adjust to rising sea level through biotic controls on change in soil elevation. Glob. Ecol. Biogeogr. 16, 545–556. https://doi.org/10.1111/j.1466-8238.2007.00317.x.
McManus, J., 2002. Deltaic responses to changes in river regimes. Mar. Chem. 79, 155–170. https://doi.org/10.1016/S0304-4203(02)00061-0.
Meade, R.H., Moody, J.A., 2010. Causes for the decline of suspended-sediment discharge in the Mississippi River system, 1940–2007. Hydrol. Process. 24, 35–49. https://doi.org/10.1002/hyp.7477.
Milliman, J.D., Farnsworth, K.L., 2011. River Discharge to the Coastal Ocean: A Global Synthesis. Cambridge University Press, Cambridge, UK, pp. 1–383. https://doi.org/10.1017/CBO9780511781247.
Mirza, M.M., 1998. Diversion of the Ganges water at Farakka and its effects on salinity in Bangladesh. Environ. Manage. 22, 711–722. https://doi.org/10.1007/s002679900141.
Morris, J.T., Sundareshwar, P.V., Nietch, C.T., Kjerfve, B., Cahoon, D.R., 2002. Responses of coastal wetlands to rising sea level. Ecology 83, 2869–2877. https://doi.org/10.1890/0012-9658(2002) 083%5B2869:ROCWTR%5D2.0.CO;2.
Nelson, J.D., Miller, D.J., 1992. Expansive Soils: Problem and Practice in Foundation and Pavement Engineering. Wiley, New York.
Neubauer, S.C., 2008. Contributions of mineral and organic components to tidal freshwater marsh accretion. Estuar. Coast. Shelf Sci. 78, 78–88. https://doi.org/10.1016/j.ecss.2007.11.011.
Nicholls, R.J., Wong, P.P., Burkett, V., Codignotto, J., Hay, J., McLean, R., 2007. Coastal systems and low lying areas. In: Parry, M.L., Canziani, O.F., Palutikof, J.P., van der Linden, P.J., Hanson, C.E. (Eds.), Climate Change 2007: Impacts, Adaptation, and Vulnerability, Contribution of Working Group II to the Fourth Assessment Report of the Intergovernmental Panel on Climate Change. Cambridge University Press, Cambridge, UK, pp. 315–357.
Nuttle, W.K., Hemand, H.F., 1988. Salt marsh hydrology: implications for biogeochemical fluxes to the atmosphere and estuaries. Glob. Biogeochem. Cycl. 2, 91–114. https://doi.org/10.1029/GB002i002p00091.
Nuttle, W.K., Hemond, H.F., Stolzenbach, K.D., 1990. Mechanisms of water storage in salt marsh sediments: the importance of dilation. Hydrol. Process. 4, 1–13. https://doi.org/10.1002/hyp.3360040102.
Nyman, J.A., Walters, R.J., Delaune, R.D., Patrick Jr., W.H., 2006. Marsh vertical accretion via vegetative growth. Estuar. Coast. Shelf Sci. 69, 370–380. https://doi.org/10.1016/j.ecss.2006.05.041.
Orton, G.J., Reading, H.G., 1993. Variability of deltaic processes in terms of sediment supply, with particular emphasis on grain size. Sedimentology 40, 475–512. https://doi.org/10.1111/j.1365-3091.1993.tb01347.x.
Pethick, J., 2012. Assessing Changes in the Landform and Geomorphology Due to Sea Level Rise in the Bangladesh Sundarbans. Report to World Bank, pp. 1–42.
Pethick, J., Orford, J.D., 2013. Rapid rise in effective sea-level in southwest Bangladesh: its causes and contemporary rates. Global Planet. Change 111, 237–245. https://doi.org/10.1016/j.gloplacha.2013.09.019.
Peyronnin, N., Green, M., Richards, C.P., Owens, A., Reed, D., Chamberlain, J., et al., 2013. Louisiana's 2012 Coastal Master Plan: overview of a science-based and publicly informed decision-making process. J. Coast. Res. 67, 1–5. https://doi.org/10.2112/SI_67_1.1.
Rogers, K., Wilton, K.M., Saintilan, N., 2006. Vegetation change and surface elevation dynamics in estuarine wetlands of southeast Australia. Estuar. Coast. Shelf Sci. 66, 559–569. https://doi.org/10.1016/j.ecss.2005.11.004.
Rogers, K., Saintilan, N., 2008. Relationships between surface elevation and groundwater in mangrove forests of southeast Australia. J. Coast. Res. 24, 63–69. https://doi.org/10.2112/05-0519.1.
Rogers, K.G., Goodbred, S.L., Mondal, D.R., 2013. Monsoon sedimentation on the 'abandoned' tide-influenced Ganges-Brahmaputra delta plain. Estuar. Coast. Shelf Sci. 131, 297–309. https://doi.org/10.1016/j.ecss.2013.07.014.
Rogers, K.G., Goodbred, S.L., 2014. The Sundarbans and Bengal Delta: the world's largest tidal mangrove and delta system. In: Landscapes and Landforms of India. Springer, Dordrecht, pp. 181–187. https://doi.org/10.1007/978-94-017-8029-2_18.
Rogers, K.G., Overeem, I., 2017. Doomed to drown? Sediment dynamics in the human-controlled floodplains of the active Bengal Delta. Elementa 5, 1–15. https://doi.org/10.1525/elementa.250.
Rovai, A.S., Twilley, R.R., Castañeda-Moya, E., Riul, P., Cifuentes-Jara, M., Manrow-Villalobos, M., Horta, P.A., Simonassi, J.C., Fonseca, A.L., Pagliosa, P.R., 2018. Global controls on carbon storage in mangrove soils. Nat. Clim. Change 8, 534. https://doi.org/10.1038/s41558-018-0162-5.

Sadler, P.M., 1981. Sediment accumulation rates and the completeness of stratigraphic sections. J. Geol. 89, 569–584. https://doi.org/10.1086/628623.
Sasmito, S.D., Murdiyarso, D., Friess, D.A., Kurnianto, S., 2016. Can mangroves keep pace with contemporary sea level rise? A global data review. Wetlands Ecol. Manage. 24, 263–278. https://doi.org/10.1007/s11273-015-9466-7.
Schafer, W.M., Singer, M.J., 1976. Influence of physical and mineralogical properties on swelling of soils in Yolo County, California. Soil Sci. Soc. Am. J. 40, 557–562.
Shaha, D.C., Cho, Y.K., 2016. Salt plug formation caused by decreased river discharge in a multi-channel estuary. Sci. Rep. 6, 1–11. https://doi.org/10.1038/srep27176.
Steckler, M.S., Nooner, S.L., Akhter, S.H., Chowdhury, S.K., Bettadpur, S., Seeber, L., Kogan, M.G., 2010. Modeling Earth deformation from monsoonal flooding in Bangladesh using hydrographic, GPS, and Gravity Recovery and Climate Experiment (GRACE) data. J. Geophys. Res. Solid Earth 115, B8.
Steiger, J., Gurnell, A.M., Goodson, J.M., 2003. Quantifying and characterizing contemporary riparian sedimentation. River Res. Appl. 19, 335–352. https://doi.org/10.1002/rra.708.
Syvitski, J.P., Saito, Y., 2007. Morphodynamics of deltas under the influence of humans. Glob. Planet. Change 57, 261–282. https://doi.org/10.1016/j.gloplacha.2006.12.001.
Syvitski, J.P., Kettner, A.J., Overeem, I., Hutton, E.W., Hannon, M.T., Brakenridge, G.R., et al., 2009. Sinking deltas due to human activities. Nat. Geosci. 2, 681–686. https://doi.org/10.1038/ngeo629.
Tessler, Z.D., Vörösmarty, C.J., Grossberg, M., Gladkova, I., Aizenman, H., Syvitski, J.P., et al., 2015. Profiling risk and sustainability in coastal deltas of the world. Science 349, 638–643. https://doi.org/10.1126/science.aab3574.
Törnqvist, T.E., Bridge, J.S., 2002. Spatial variation of overbank aggradation rate and its influence on avulsion frequency. Sedimentology 49, 891–905. https://doi.org/10.1046/j.1365-3091.2002.00478.x.
Törnqvist, T.E., Wallace, D.J., Storms, J.E., Wallinga, J., Van Dam, R.L., Blaauw, M., et al., 2008. Mississippi Delta subsidence primarily caused by compaction of Holocene strata. Nat. Geosci. 1, 173. https://doi.org/10.1038/ngeo129.
Van Asselen, S., Stouthamer, E., Van Asch, T.W., 2009. Effects of peat compaction on delta evolution: a review on processes, responses, measuring and modeling. Earth Sci. Rev. 92, 35–51. https://doi.org/10.1016/j.earscirev.2008.11.001.
Van Coppenolle, R., Schwarz, C., Temmerman, S., 2018. Contribution of mangroves and salt marshes to nature-based mitigation of coastal flood risks in major deltas of the world. Estuar. Coasts 41, 1699–1711. https://doi.org/10.1007/s12237-018-0394-7.
Van Santen, P., Augustinuus, P.G.E.F., Janssen-Stelder, M.M., Quartel, S., Tri, N.H., 2007. Sedimentation in an estuarine mangrove swamp. J. Asian Earth Sci. 29, 566–575. https://doi.org/10.1016/j.jseaes.2006.05.011.
Vörösmarty, C.J., Syvitski, J., Day, J., de Sherbinin, A., Giosan, L., Paola, C., 2009. Battling to save the world's river deltas. Bull. Atom. Sci. 65, 31–43. https://doi.org/10.2968/065002005.
Wang, H., Yang, Z., Saito, Y., Liu, J.P., Sun, X., 2007. Stepwise decreases of the Huanghe (Yellow River) sediment load (1950–2004): impacts from climate changes and human activities. Glob. Planet Change 57, 331–354.
Whelan, K.R., Smith, T.J., Cahoon, D.R., Lynch, J.C., Anderson, G.H., 2005. Groundwater control of mangrove surface elevation: shrink and swell varies with soil depth. Estuaries 28, 833–843. https://doi.org/10.1007/BF02696013.
Wilson, C.A., Goodbred, S.L., 2015. Construction and maintenance of the Ganges-Brahmaputra-Meghna delta: linking process, morphology, and stratigraphy. Ann. Rev. Mar. Sci. 7, 67–88. https://doi.org/10.1146/annurev-marine-010213-135032.
Wilson, C.A., Goodbred, S.L., Small, C., Gilligan, J.M., Sams, S., 2017. Widespread infilling of tidal channels and navigable waterways in the human-modified tidal deltaplain of southwest Bangladesh. Elementa 5, 1–12. https://doi.org/10.1525/elementa.263.
Winterwerp, J.C., Giardino, A., 2012. Assessment of Increasing Freshwater Input on Salinity and Sedimentation in the Gorai River System. Deltares, Netherlands, pp. 1–63.
Winterwerp, J.C., Van Kesteren, W.G., 2004. Introduction to the Physics of Cohesive Sediment Dynamics in the Marine Environment, vol. 56 Elsevier.
Wolanski, E., Moore, K., Spagnol, S., D'Adamo, N., Pattiaratchi, C., 2001. Rapid, human-induced siltation of the macro-tidal Ord River estuary, Western Australia. Estuar. Coast. Shelf Sci. 53, 717–732. https://doi.org/10.1006/ecss.2001.0799.
Woodroffe, C.D., Rogers, K., McKee, K.L., Lovelock, C.E., Mendelssohn, I.A., Saintilan, N., 2016. Mangrove sedimentation and response to relative sea-level rise. Ann. Rev. Mar. Sci. 8, 243–266. https://doi.org/10.1146/annurev-marine-122414-034025.
World Bank, 2015. Bangladesh morphology and climate adaptation, Coastal Embankment Improvement Project, Phase-I (CEIP-I): Long term monitoring, research and analysis of Bangladesh coastal zone (sustainable polders adapted to coastal dynamics). Technical Proposal to Bangladesh Water Development Board (BWDB), December 2015.